

Investigation on Photovoltaic Performance based on Matchstick-Like Cu_2S – In_2S_3 Heterostructure Nanocrystals and Polymer

Aiwei Tang · Feng Teng · Yan Wang ·
Yanbing Hou · Wei Han · Luoxin Yi ·
Mingyuan Gao

Received: 11 August 2008 / Accepted: 3 October 2008 / Published online: 25 October 2008
© to the authors 2008

Abstract In this paper, we synthesized a novel type II cuprous sulfide (Cu_2S)–indium sulfide (In_2S_3) heterostructure nanocrystals with matchstick-like morphology in pure dodecanethiol. The photovoltaic properties of the heterostructure nanocrystals were investigated based on the blends of the nanocrystals and poly(2-methoxy-5-(2'-ethylhexoxy)-*p*-phenylenevinylene) (MEH-PPV). In comparison with the photovoltaic properties of the blends of Cu_2S or In_2S_3 nanocrystals alone and MEH-PPV, the power conversion efficiency of the hybrid device based on blend of Cu_2S – In_2S_3 and MEH-PPV is enhanced by ~ 3 – 5 times. This improvement is consistent with the improved exciton dissociation or separation and better charge transport abilities in type II heterostructure nanocrystals.

Keywords Photovoltaic performance · Heterostructure nanocrystals · Cu_2S – In_2S_3 · MEH-PPV · Charge-transfer

Introduction

Since 1996, Greenham et al [1] reported the photovoltaic device based on inorganic nanocrystals and conjugated polymer; hybrid photovoltaic devices fabricated by incorporating inorganic nanocrystals (such as CdSe [2–4], CdS [5], $\text{CdSe}_x\text{Te}_{1-x}$ [6], CuInS_2 [7], ZnO [8, 9], TiO_2 [10, 11], PbS [12], and so on) into conjugated polymer matrixes have been extensively studied. This has been demonstrated that the performance of the hybrid photovoltaic devices could be enhanced by using the blends of these different-shaped inorganic nanocrystals and conjugated polymers [13, 14]. In these hybrid devices, the photo-induced charge transfer is favored between inorganic nanocrystals with high electron affinity and conjugated polymers with relatively low ionization potential. The neutral excitons in polymer and nanocrystals produced by photo-excitation are separated into free carriers at the nanocrystal/polymer interface and then are transported through their own pathways to the electrode, resulting in the generation of photocurrent and photo-voltage [15, 16].

Currently, a significant interest has been directed toward the design of semiconductor heterostructure nanocrystals for electroluminescence and photovoltaic applications [15, 16]. The semiconductor heterostructure nanocrystals, composed of at least two different types of materials with different band-gaps, can be generally classified into two types according to the electronic structures built up within the heterostructures. With respect to type I heterostructure, the mismatch between the energetic levels of each component is unfavorable for exciton dissociation, while type II heterostructure is in favor of charge separation upon photo-irradiation. Thus, type II heterostructure nanocrystals are believed to be useful for photovoltaic applications [15, 17]. There have been several reports on the synthesis of type II

A. Tang · F. Teng · Y. Wang · Y. Hou (✉)
Key Laboratory of Luminescence and Optical Information,
Ministry of Education, Institute of Optoelectronic Technology,
Beijing JiaoTong University, Beijing 100044,
People's Republic of China
e-mail: ybhhou@bjtu.edu.cn

A. Tang
e-mail: awtangbjtu@yahoo.com.cn

W. Han · L. Yi · M. Gao (✉)
Institute of Chemistry, Chinese Academy of Sciences,
Zhong Guan Cun, Bei Yi Jie 2, Beijing 100080,
People's Republic of China
e-mail: gaomy@iccas.ac.cn

heterostructure nanocrystals, containing heavy metal such as cadmium or lead ions [15, 18, 19]. However, there are very few reports about the investigation of the photovoltaic properties on the type II heterostructure nanocrystals to date. Furthermore, taking the environmental problems into consideration, environmental friendly nanocrystals containing copper and indium should be more welcome for their applications in photovoltaic devices.

Cu_{2-x}S is a *p*-type semiconductor possessing an *x*-dependent band-gap energy varying from ~ 1.2 eV for chalcocite ($x = 0$) to ~ 1.5 eV for digenite ($x = 0.2$), accompanied by a transformation from an indirect-gap semiconductor to a direct one, and it has high absorption coefficient of about 10^5 cm^{-1} (at 750 nm) [20]. In contrast, In_2S_3 is an important *n*-type semiconducting material with a band-gap as narrow as 2.00–2.30 eV, which presents both direct and indirect conduction-to-valence transitions [21].

Herein, we report a new type II matchstick-like Cu_2S – In_2S_3 heterostructure nanocrystals, synthesized by successively pyrolyzing copper (II) acetylacetonate ($\text{Cu}(\text{acac})_2$) and indium acetylacetonate ($\text{In}(\text{acac})_3$) in pure dodecanethiol, which is nontoxic and environmental friendly. Furthermore, we fabricated the hybrid photovoltaic devices using the blends of the Cu_2S – In_2S_3 nanocrystals and poly(2-methoxy-5-(2'-ethylhexoxy)-*p*-phenylenevinylene) (MEH-PPV). To study the photovoltaic performance of the Cu_2S – In_2S_3 /MEH-PPV films related to the built-in heterostructures, the photovoltaic performance of the single component spherical Cu_2S nanocrystals and In_2S_3 nanorods were also investigated.

Experimental Section

Synthesis of Nanocrystals

Cu_2S nanocrystals, Cu_2S – In_2S_3 heterostructure nanocrystals, and In_2S_3 nanorods were synthesized in our laboratory, and more details of the synthesis and characterizations are published elsewhere [22]. All the synthetic processes were carried out under the protection of nitrogen gas. The synthesis of spherical Cu_2S nanocrystals was accomplished by directly decomposing the dodecanethiol solution of $\text{Cu}(\text{acac})_2$ at the temperature of 200 °C. The matchstick-like Cu_2S – In_2S_3 heterostructure nanocrystals were prepared as follows: the organometallic $\text{Cu}(\text{acac})_2$ was firstly pyrolyzed in pure dodecanethiol at 200 °C for several minutes, and three portions of dodecanethiol solutions containing $\text{In}(\text{acac})_3$ were intermittently injected into the $\text{Cu}(\text{acac})_2$ dodecanethiol solution without stopping the heating process. The In_2S_3 nanorods were prepared by chemically detaching the Cu_2S segment from the matchstick-like Cu_2S – In_2S_3 heterostructure nanocrystals by

introducing 1,10-phenanthroline into the reaction system, and the reaction was allowed to take place at room temperature under magnetic stirring. The purification procedures of the samples were carried out by adding appropriate amount of ethanol into the samples and centrifuging at 4000 rpm for 10 min. After that, the precipitates were collected and washed twice with chloroform to remove precursor and surfactant residuals. Finally, the samples were re-dissolved into chloroform for TEM characterization.

Device Fabrication

The hybrid nanocrystal/polymer photovoltaic devices were fabricated as follows: A piece of indium–tin-oxide (ITO) glass substrates was cleaned and used as the anode. A layer of poly(3,4-ethylene dioxythiophene):poly(styrene sulfonate) (PEDOT:PSS) was spin-coated onto the treated ITO substrate and was baked at 150 °C for about 10 min. Afterwards, different chloroform solutions containing 10 wt% of Cu_2S – In_2S_3 heterostructure nanocrystals and 5 mg/mL MEH-PPV were prepared and spin-coated onto the PEDOT:PSS layer. After that, a thin layer of aluminum electrode was thermally evaporated in vacuum and used as the cathode. To provide experimental support for the use of Cu_2S – In_2S_3 heterostructure nanocrystals, similarly structured hybrid photovoltaic devices were prepared through replacing Cu_2S – In_2S_3 heterostructure nanocrystals by spherical copper sulfide nanocrystals and In_2S_3 nanorods with the mass concentration of 10 wt% in the blends. The photoactive area of the device was about 9 mm^2 . The chemical structure of MEH-PPV and the hybrid photovoltaic device structure are shown in Fig. 1a and b, respectively.

Measurements

Dimensions and morphologies of spherical Cu_2S nanocrystals, matchstick-like Cu_2S – In_2S_3 heterostructure nanocrystals, and In_2S_3 nanorods were characterized by

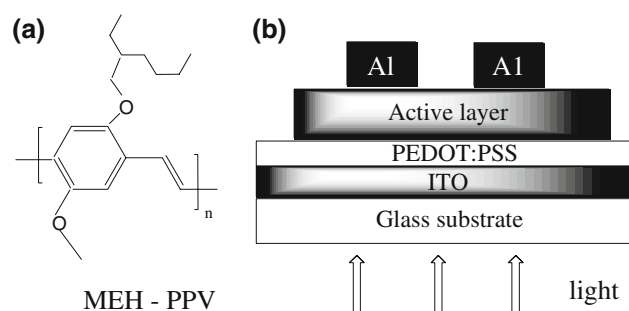


Fig. 1 a Chemical structure of MEH-PPV; b Schematic illustration of the hybrid photovoltaic device structure

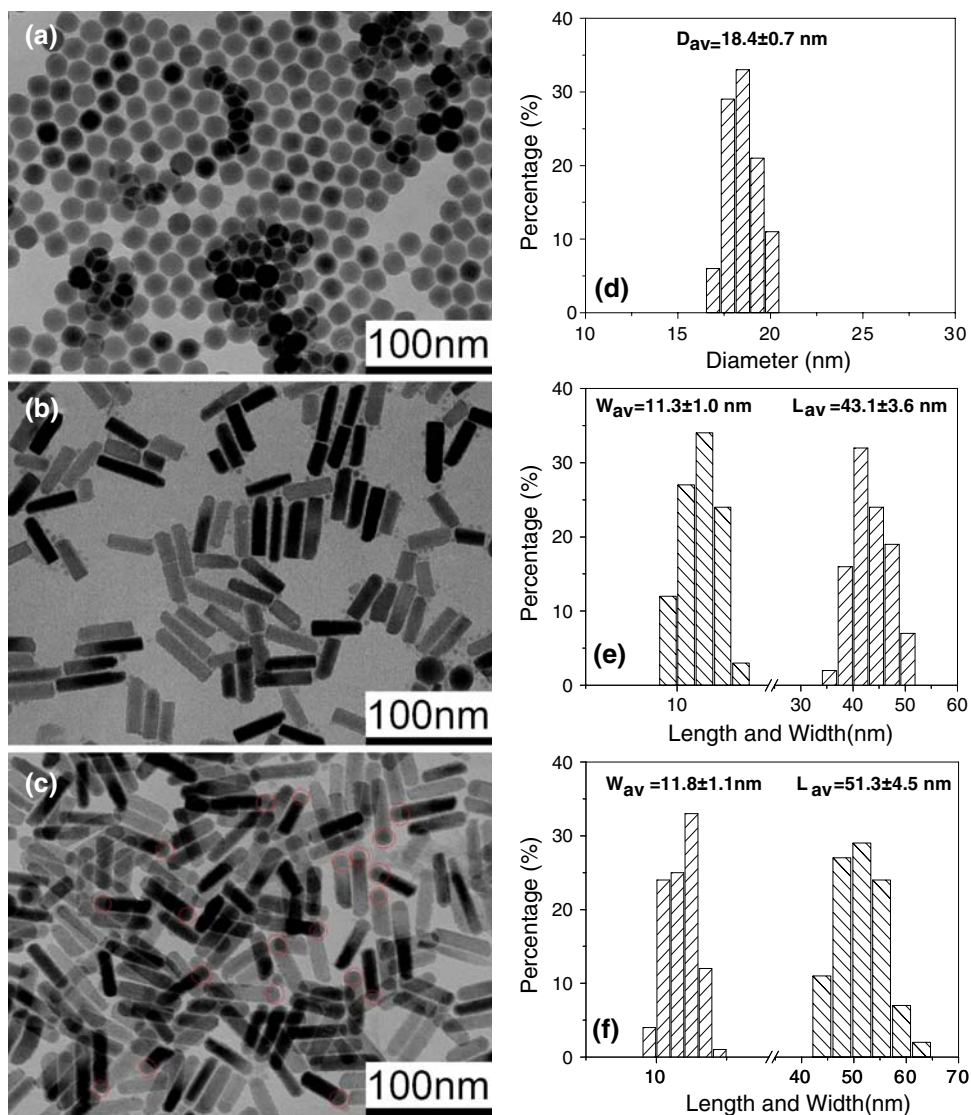
transmission electron microscopy (TEM), and were recorded with a JEM-100CXII electron microscope operating at an accelerating voltage of 100 kV. TEM samples were prepared by dropping a dilute solution of the samples in chloroform on carbon-coated copper grids and then allowing the solvent to evaporate. Mean diameters, lengths, and widths were determined by counting at least 300 particles per sample for statistical purposes. Powder X-ray diffraction (XRD) were obtained with a Regaku D/Max-2500 diffractometer equipped with a Cu $K\alpha 1$ radiation ($\lambda = 1.54056 \text{ \AA}$). The current density–voltage (J – V) characteristics of the photovoltaic devices were measured using a Keithley 2410 source measure unit both in dark and under illumination at 500 nm. Monochromatic illumination was produced by the output of a xenon lamp dispersed by a monochromator in SPEX Fluorolog-3 spectrophotometer.

Results and Discussions

The transmission electron microscopy (TEM) images of spherical Cu_2S nanoparticles, In_2S_3 nanorods, and matchstick-like Cu_2S – In_2S_3 heterostructure nanocrystals are shown in Fig. 2a–c, respectively, and the corresponding size distribution histogram of the obtained nanocrystals are shown in Fig. 2d–f. The mean diameter of copper sulfide nanocrystals is calculated to be about $18.4 \pm 0.7 \text{ nm}$, and the length and width of the In_2S_3 nanorods are $43.1 \pm 3.6 \text{ nm}$ and $11.3 \pm 1.0 \text{ nm}$, respectively. For the matchstick-like Cu_2S – In_2S_3 nanocrystals, the mean length and width are measured to be $51.3 \pm 4.5 \text{ nm}$ and $11.8 \pm 1.1 \text{ nm}$, respectively.

Figure 3 gives the XRD pattern of the matchstick-like Cu_2S – In_2S_3 heterostructure nanocrystals, which further

Fig. 2 TEM images of **a** Cu_2S nanocrystals, **b** In_2S_3 nanorods, and **c** matchstick-like Cu_2S – In_2S_3 heterostructure nanocrystals (part of the heads are marked by the red circle). The panels **(d)**, **(e)**, and **(f)** correspond to the size distribution histograms of the samples used in our work



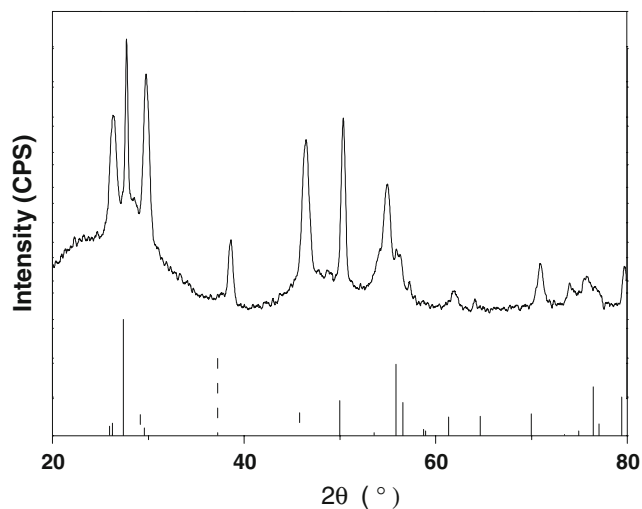


Fig. 3 XRD pattern of the matchstick-like heterostructure nanocrystals. The solid and dash lines shown in below the frame correspond to the standard In_2S_3 (JCPDS: 73-1366) and Cu_2S (JCPDS: 84-0206), respectively

confirms the matchstick-like heterostructure nanocrystals are indeed made of the discrete Cu_2S and In_2S_3 rather than the single crystal of CuInS_2 or something else. The XRD result indicates that the matchstick-like heterostructure nanocrystals is undoubtedly constructed by Cu_2S and In_2S_3 nanocrystals.

We performed current density (J)–voltage (V) measurements for the as-fabricated hybrid photovoltaic device with such a structure: ITO/PEDOT:PSS/ Cu_2S – In_2S_3 (10 wt%):MEH-PPV/Al. Figure 4 corresponds to the representative J – V characteristics recorded in the dark and under illumination of 16.7 mW cm^{-2} monochromatic xenon light at 500 nm. It can be seen that there is no current response in the dark and a significant photovoltaic effect under illumination. Under illumination, we got a short-circuit current density (J_{SC}) of $76.9 \mu\text{A cm}^{-2}$ and an open-circuit voltage (V_{OC}) of 0.72 V, and the fill factor (FF) of 0.295, which gave a power conversion efficiency of 0.1%. This result is comparable with that of the photovoltaic devices based on similar nanocrystals such as CuInS_2 or Cu_2S -Carbon nanotube heterostructure nanostructures [7, 16]. A better device performance can be expected by optimizing the device structures, such as increasing the mass concentration of nanocrystals in the blends, optimizing the device structure, or annealing the device at proper temperatures; and the related studies in our laboratory are in progress.

The general photovoltaic performances of the hybrid devices containing 10 wt% Cu_2S – In_2S_3 matchstick-like nanocrystals were investigated by comparing with the devices in which the matchstick-like nanocrystals were replaced by either spherical Cu_2S nanoparticles or In_2S_3

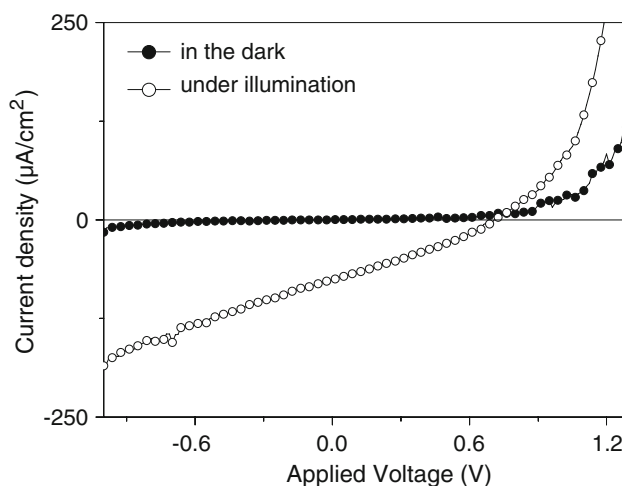


Fig. 4 Current density–voltage characteristics of the MEH-PPV: Cu_2S – In_2S_3 hybrid device in the dark (closed circles) and under illumination (open circles)

nanorods. The J – V characterizations of these devices based on the hybrid films and pristine MEH-PPV film were measured in the dark and under illumination, and the results are shown in Fig. 5. From these J – V curves, we obtained the device parameters (J_{sc} , V_{oc} , FF, and η) for the different photovoltaic devices, which are summarized in Table 1. The power conversion efficiency of the hybrid nanocrystal/polymer devices are all improved relative to that of the pristine MEH-PPV device, which can be attributed to the better charge separation/transfer at the polymer/nanocrystal interface and the better charge transport in the composite systems. It is notable that the power conversion efficiency of the hybrid Cu_2S – In_2S_3 :MEH-PPV photovoltaic device is enhanced 3–5 times as compared to that of the hybrid devices based on the single-component nanocrystals. This suggests that the dissociation probability of the photo-generated excitons is enhanced in the hybrid photovoltaic devices based on type II heterostructure nanocrystals as compared to those based on single-composition nanocrystals. Unfortunately, we cannot offer a firm explanation for the enhanced power conversion efficiency of the Cu_2S – In_2S_3 :MEH-PPV hybrid devices; however, the possible origin of these observations can be understood on the basis of the energy level diagram of the hybrid device ITO/PEDOT:PSS/ Cu_2S – In_2S_3 :MEH-PPV/Al.

Figure 6 shows the energy diagram of the valence- and conduction-band levels, which illustrates the charge-transfer junction between the Cu_2S , In_2S_3 , MEH-PPV, PEDOT/PSS, ITO, and Al electrodes. Herein, the band-gap and Fermi level of Cu_2S and In_2S_3 are obtained from the previous reports [16, 23]. It is seen that the nanocrystal is an electron acceptor and MEH-PPV a hole acceptor. When the photons are absorbed by the nanocrystal/MEH-PPV

Fig. 5 Current density–voltage curves in the dark (*closed circles*) and under illumination (*open circles*) of the samples **a** MEH-PPV; **b** MEH-PPV:Cu₂S (10 wt%); **c** MEH-PPV:In₂S₃ (10 wt%); **d** MEH-PPV: Cu₂S–In₂S₃ (10 wt%), in which the current density is expressed in logarithmic coordinates

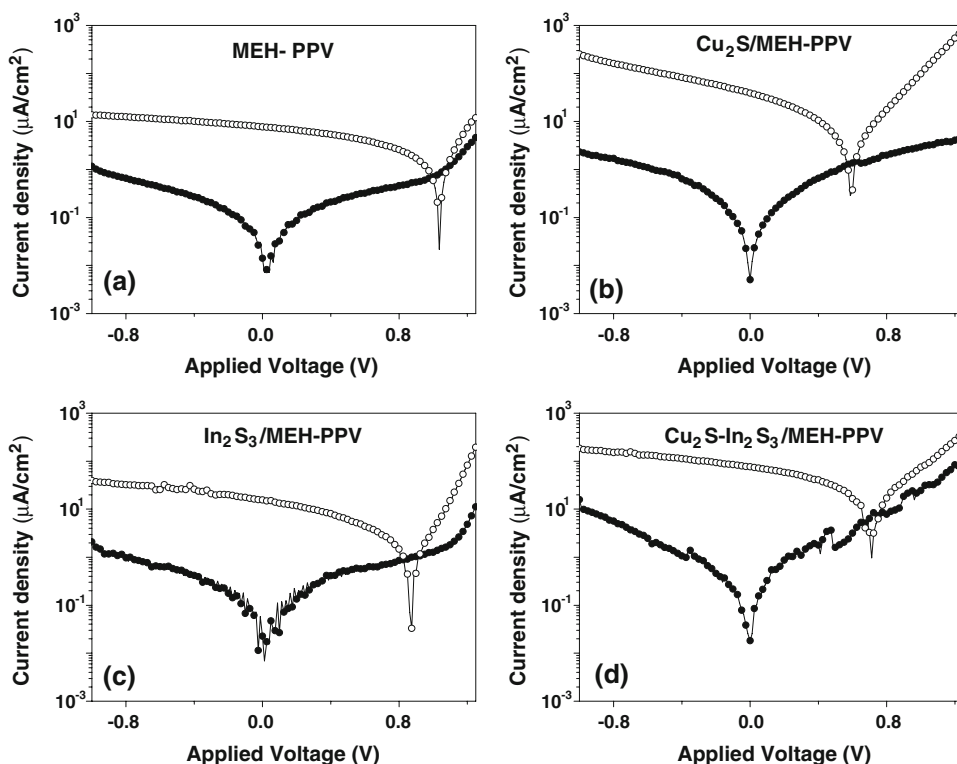


Table 1 Summary of device parameters for the photovoltaic devices using pristine MEH-PPV, MEH-PPV:Cu₂S, MEH-PPV:In₂S₃, and MEH-PPV:Cu₂S–In₂S₃ as active layers under illumination

Active layer	I_{sc} ($\mu A\ cm^{-2}$)	V_{oc} (V)	FF	η (%)
Pristine MEH-PPV	7.82	1.04	0.251	0.015
Cu ₂ S:MEH-PPV	39.7	0.59	0.214	0.03
In ₂ S ₃ :MEH-PPV	15.5	0.87	0.239	0.02
Cu ₂ S–In ₂ S ₃ :MEH-PPV	76.9	0.72	0.295	0.10

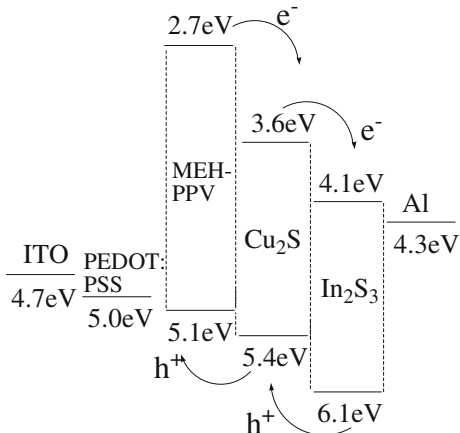


Fig. 6 Energy level diagram showing the charge transfer for the MEH-PPV:Cu₂S–In₂S₃ hybrid photovoltaic device

composites, the excitons are formed in both nanocrystals and MEH-PPV phase. Then the excitons migrate to the nanocrystal/polymer interface, followed by the exciton dissociation into holes and electrons. The resulting electrons and holes can be transported to cathode and anode to generate photocurrent and photo-voltage. Generally, the nanocrystal is expected to be used as the electron transport channel whereas the polymer is the path for the hole transport path. But for the heterostructure Cu₂S–In₂S₃ nanocrystals, the In₂S₃ can serve as a more efficient electron acceptor from the excited Cu₂S nanocrystals. For the Cu₂S–In₂S₃ heterostructure nanocrystals, the photons can be absorbed by either part or intermediate states that exist at the junction between the two materials [15]. When the excitons are formed in either part, the exciton dissociation into electrons and holes at the interface of Cu₂S (as donor)/In₂S₃ (as acceptor) will occur. Because the Cu₂S or In₂S₃ part helps to transport holes or electrons to the opposite electrodes, the charge separation will be quickened and the recombination process will be impeded. That is, the highly conductive In₂S₃ part provides direct and efficient paths for the transport of conduction-band electrons to the cathode [16]. As compared to the photovoltaic devices based on the blends of only Cu₂S or In₂S₃ and MEH-PPV, the exciton dissociation and charge transportation become more efficient in the hybrid device based on Cu₂S–In₂S₃ heterostructures and MEH-PPV.

Conclusions

In summary, we studied the photovoltaic properties of the hybrid devices based on the blends of MEH-PPV and the type II Cu_2S – In_2S_3 heterostructure nanocrystals, which are environmental friendly and nontoxic. As compared to the hybrid device using single-composition Cu_2S or In_2S_3 , the power conversion efficiency of the Cu_2S – In_2S_3 :MEH-PPV device showed an obvious improvement, which could be attributed to higher exciton dissociation probability and more efficient charge transportation in type II heterostructure nanocrystals. This work may supply a new environmental friendly and type II heterostructure nanocrystals to design candidate materials for hybrid photovoltaic devices.

Acknowledgments The authors gratefully acknowledge the financial support of National Key Project of Basic Research of China (No. 2003CB314707), National Natural Science Foundation of China (Nos. 10434030 and 90401006), Key Project of Chinese Ministry of Education (No. 105041). The author (Aiwei Tang) is also grateful to the Doctor Innovation Foundation of Beijing Jiaotong University (No. 48023).

References

1. N.C. Greenham, X.G. Peng, A.P. Alivisatos, *Phys. Rev. B* **54**, 17628 (1996). doi:[10.1103/PhysRevB.54.17628](https://doi.org/10.1103/PhysRevB.54.17628)
2. W.U. Huynh, J.J. Dittmer, A.P. Alivisatos, *Science* **295**, 2425 (2003). doi:[10.1126/science.1069156](https://doi.org/10.1126/science.1069156)
3. B.Q. Sun, E. Marx, N.C. Greenham, *Nano Lett.* **3**, 961 (2003). doi:[10.1021/nl0342895](https://doi.org/10.1021/nl0342895)
4. A.W. Tang, F. Teng, H. Jin, Y.H. Gao, Y.B. Hou, C.J. Liang, Y.S. Wang, *Mater. Lett.* **61**, 2178 (2007). doi:[10.1016/j.matlet.2006.08.042](https://doi.org/10.1016/j.matlet.2006.08.042)
5. L. Wang, Y.S. Liu, X. Jiang, D.H. Qin, Y. Cao, *J. Phys. Chem. C* **111**, 9538 (2007). doi:[10.1021/jp0715777](https://doi.org/10.1021/jp0715777)
6. Y. Zhou, Y.C. Li, H.Z. Zhong, J.H. Hou, Y.Q. Ding, C.H. Yang, Y.F. Li, *Nanotechnology* **17**, 4041 (2006). doi:[10.1088/0957-4484/17/16/008](https://doi.org/10.1088/0957-4484/17/16/008)
7. E. Arici, S. Sariciftci, D. Meissner, *Adv. Funct. Mater.* **13**, 165 (2003). doi:[10.1002/adfm.200390024](https://doi.org/10.1002/adfm.200390024)
8. W.J.E. Beek, L.H. Slooff, M.M. Wienk, J.M. Kroon, R.A.J. Janssen, *Adv. Funct. Mater.* **15**, 1703 (2005). doi:[10.1002/adfm.200500201](https://doi.org/10.1002/adfm.200500201)
9. W.J.E. Beek, M.M. Wienk, M. Kemerink, X.N. Yang, R.A.J. Janssen, *J. Phys. Chem. B* **109**, 9505 (2005). doi:[10.1021/jp050745x](https://doi.org/10.1021/jp050745x)
10. P. Ravirajan, S.A. Haque, J.R. Durrant, D.D.C. Bradley, J. Nelson, *Adv. Funct. Mater.* **15**, 609 (2005). doi:[10.1002/adfm.200400165](https://doi.org/10.1002/adfm.200400165)
11. K. Shankar, G.K. Mor, H.E. Prakasam, O.K. Varghese, C.A. Grimes, *Langmuir* **23**, 12445 (2007). doi:[10.1021/la7020403](https://doi.org/10.1021/la7020403)
12. S.A. McDonald, P.W. Cyr, L. Levina, E.H. Sargent, *Appl. Phys. Lett.* **85**, 2089 (2004). doi:[10.1063/1.1792380](https://doi.org/10.1063/1.1792380)
13. I. Gur, N.A. Fromer, C.-P. Chen, A.G. Kanaras, A.P. Alivisatos, *Nano Lett.* **7**, 409 (2007). doi:[10.1021/nl062660t](https://doi.org/10.1021/nl062660t)
14. B.Q. Sun, N.C. Greenham, *Phys. Chem. Chem. Phys.* **8**, 3557 (2006). doi:[10.1039/b604734n](https://doi.org/10.1039/b604734n)
15. H.Z. Zhong, Y. Zhou, Y. Yang, C.H. Yang, Y.F. Li, *J. Phys. Chem. C* **111**, 6538 (2007). doi:[10.1021/jp0709407](https://doi.org/10.1021/jp0709407)
16. H. Lee, S.W. Yoon, E.J. Kim, J. Park, *Nano Lett.* **7**, 778 (2007). doi:[10.1021/nl0630539](https://doi.org/10.1021/nl0630539)
17. P.D. Cozzoli, T. Pellegrino, L. Manna, *Chem. Soc. Rev.* **35**, 1195 (2006). doi:[10.1039/b517790c](https://doi.org/10.1039/b517790c)
18. D.J. Milliron, S.M. Hughes, Y. Cui, L. Manna, J.B. Li, L.-W. Wang, A.P. Alivisatos, *Nature* **430**, 190 (2004). doi:[10.1038/nature02695](https://doi.org/10.1038/nature02695)
19. D.V. Talapin, R. Koeppel, S. Götzinger, A. Kornowski, J.M. Lupton, A.L. Rogach, O. Benson, J. Feldmann, H. Weller, *Nano Lett.* **3**, 1677 (2003). doi:[10.1021/nl034815s](https://doi.org/10.1021/nl034815s)
20. V.I. Klimov, V.A. Karavanskii, *Phys. Rev. B* **54**, 8087 (1996). doi:[10.1103/PhysRevB.54.8087](https://doi.org/10.1103/PhysRevB.54.8087)
21. D.K. Nagesha, X. Liang, A.A. Mamedov, G. Gainer, M.A. Eastman, M. Giersig, J.-J. Song, T. Ni, N.A. Kotov, *J. Phys. Chem. B* **105**, 7490 (2001). doi:[10.1021/jp011265i](https://doi.org/10.1021/jp011265i)
22. W. Han, L.X. Yi, N. Zhao, A.W. Tang, M.Y. Gao, Z.Y. Tang, *J. Am. Chem. Soc.* **130**, 13152 (2008). doi:[10.1021/ja8046393](https://doi.org/10.1021/ja8046393)
23. Y. Yasaki, N. Sonoyama, T. Sakata, *J. Electroanal. Chem.* **469**, 116 (1999). doi:[10.1016/S0022-0728\(99\)00184-9](https://doi.org/10.1016/S0022-0728(99)00184-9)